Eur. Phys. J. C (2016) 76:44
DOI 10.1140/epjc/s10052-015-3867-x

THE EUROPEAN PHYSICAL JOURNAL C

CrossMark

Regular Article - Theoretical Physics

Natural NMSSM with a light Singlet Higgs and Singlino LSP

C. T. Potter[a]

Physics Department, University of Oregon, Eugene, USA

Received: 2 October 2015 / Accepted: 22 December 2015 / Published online: 25 January 2016
© The Author(s) 2016. This article is published with open access at Springerlink.com

Abstract Supersymmetry (SUSY) is an attractive extension of the Standard Model (SM) of particle physics which solves the SM hierarchy problem. Motivated by the theoretical μ-term problem of the Minimal Supersymmetric Model (MSSM), the Next-to MSSM (NMSSM) can also account for experimental deviations from the SM like the anomalous muon magnetic moment and the dark matter relic density. Natural SUSY, motivated by naturalness considerations, exhibits small fine tuning and a characteristic phenomenology with light higgsinos, stops, and gluinos. We describe a scan in NMSSM parameter space motivated by Natural SUSY and guided by the phenomenology of an NMSSM with a slightly broken Peccei–Quinn symmetry and a lightly coupled singlet. We identify a scenario which survives experimental constraints with a light singlet Higgs and a singlino lightest SUSY particle. We then discuss how the scenario is not presently excluded by searches at the Large Hadron Collider (LHC) and which channels are promising for discovery at the LHC and International Linear Collider.

1 Introduction

With the discovery of the 125 GeV Higgs boson h_{125} by ATLAS [1] and CMS [2] at the Large Hadron Collider (LHC), particle physics enters a new era. In the Standard Model (SM) of particle physics, the properties of the Higgs boson are determined by theory once the mass is known [3]. At present, their measurements are consistent with the SM prediction [4–9].

But the SM is not complete. Experimentally, it does not account for Dark Matter (DM), the anomalous muon magnetic moment or the strong CP problem, among other things. Theoretically, it suffers from the hierarchy problem. Supersymmetry (SUSY) solves the hierarchy problem by introducing a fermionic partner for each SM boson and a bosonic partner for each SM fermion [10]. SUSY with conserved R parity provides a natural candidate for DM, the Lightest Supersymmetric Partner (LSP), and it can account for the anomalous muon magnetic moment by introducing new particles in loops.

The principle of *naturalness* in physics maintains that an effective physical theory approximately valid below some characteristic scale should not be very sensitive to the correct theory above that scale [11]. Applied to electroweak symmetry breaking in SUSY, this implies that the success of the effective SM Higgs theory disallows SUSY too far above the electroweak scale [12]. In particular, the characteristic mass spectrum of *Natural* SUSY includes light superpartners of the Higgs bosons, top quark and gluon near the electroweak scale.

The Minimal SUSY Model (MSSM) contains only the SM particles and their superpartners, together with an enlarged Higgs sector: one neutral pseudoscalar, two neutral scalars and two charged scalars which arise from the two Higgs doublets $\hat{H}_u$ and $\hat{H}_d$ necessary for the Higgs mechanism in SUSY [3]. But the MSSM suffers from the so-called μ-term problem, which prevents the term $\mu \hat{H}_u \hat{H}_d$ in the MSSM superpotential from reaching the electroweak scale without fine tuning [10,13,14].

The Next-to MSSM (NMSSM) solves the μ-term problem by introducing a singlet $\hat{S}$ and replacing $\mu \hat{H}_u \hat{H}_d$ with $\lambda \hat{S} \hat{H}_u \hat{H}_d$. The Z_3 invariant NMSSM superpotential is [13,14]

$$W = \lambda \hat{S} \hat{H}_u \hat{H}_d + \frac{\kappa}{3} \hat{S}^3 \tag{1}$$

where λ and κ are free parameters. An effective μ-term is generated as the vacuum expectation value of $\hat{S}$, $\mu_{\text{eff}} = \lambda \langle \hat{S} \rangle$, reaching a natural scale without fine tuning [13,14].

In addition to the Higgs content of the MSSM, the NMSSM contains an additional pseudoscalar and an additional scalar so that the NMSSM Higgs sector consists of two neutral pseudoscalars (a_1, a_2), three neutral scalars (h_1, h_2, h_3) and two charged scalars (H^+, H^-) [15,16]. The

[a] e-mail: c.t.potter@gmail.com

NMSSM Higgs sector is fully determined at tree level by λ and κ, A_λ, and A_κ (soft trilinear couplings), $\mu_{\rm eff}$ and $\tan\beta$ (ratio of H_u, H_d vacuum expectation values) [15].

One notable version of the NMSSM is the Peccei–Quinn (PQ) symmetric NMSSM, characterized by $\kappa = 0$ [13–15,17]. The PQ symmetric NMSSM explains why there is so little CP violation in the strong sector by exhibiting an axion, the massless pseudoscalar a_1. In the NMSSM with a slightly broken PQ symmetry, with small κ and A_κ, the a_1 acquires a small mass proportional to κA_κ but can still solve the strong CP problem [15,18–21].

Scenarios with a light NMSSM pseudoscalar Higgs, motivated variously by the strong CP problem, naturalness, the anomalous muon magnetic moment, the η_b mass spectrum, and the similarity of the baryon density to the dark matter density, have been discussed in the literature [15,22–28]. In this study we assume a light NMSSM pseudoscalar a_1 with $2m_\tau < m_{a_1} < 2m_B$. Motivated by the LEP $Zb\bar{b}$ feature near $m_{b\bar{b}} \approx 60$ GeV [29], we identify this as an h_1 candidate. We further identify the h_{125} as the second lightest neutral scalar h_2 of the NMSSM and note that the h_{125} signal strength measurements at the LHC [5,6] place the heavier NMSSM a_2, h_3, H^+ in the effective MSSM decoupling limit.

2 Effective MSSM ($\lambda, \kappa \approx 0$)

We now consider the phenomenology of the NMSSM with a slightly broken PQ symmetry in which the singlet S is completely decoupled from the doublets H_u and H_d ($\lambda = 0$). We then consider how the phenomenology is altered when the singlet is allowed a weak coupling to the doublets ($\lambda \approx 0$). The case $\lambda, \kappa \approx 0$ is known as the effective MSSM [14].

For $\lambda = 0$, there is no mixing of the singlet with the doublets. The generic couplings in the NMSSM have been detailed in [14,30]. We adopt the notation of the former, denoting S^2_{ij} (P^2_{ij}) as the jth component of mass eigenstate h_i (a_i), where $j = 1, 2, 3$ corresponds to the u doublet, the d doublet, and singlet respectively. For purely singlet h_1 and a_1, $S_{13} = P_{13} = 1$, and all other S_{1j}, P_{1j} vanish, so the a_1 cannot decay to SM particles since their coupling is proportional to $P_{11} = 0$ or $P_{12} = 0$, and similarly for the h_1. The a_1 is stable and the only allowed h_1 decay for $m_{h_1} \approx 60$ GeV is $h_1 \to a_1 a_1$. The singlet sector is decoupled from the SM sector.

Furthermore, for the case $\lambda = 0$, the singlet sector is decoupled from the MSSM sector. One neutralino is pure singlino whose mass, at tree level, is related to the a_1 mass by $m_\chi = -2m^2_{a_1}/3A_\kappa$ [15,17]. For $m_{a_1} \approx 10$ GeV and $|A_\kappa|$ of $\mathcal{O}(1)$ GeV, consistent with a slightly broken PQ symmetry, this yields $m_\chi \approx 60$ GeV. In this study we identify the singlino as the LSP χ_1. Denoting N^2_{ij} as the jth component of χ_i, where $j = 1, 2, 3, 4, 5$ corresponds to bino, wino, u higgsino, d higgsino, and singlino respectively. Neutralinos heavier than the singlino LSP have a zero singlino component, $N_{15} = 1$ and all other N_{i5} vanish. No heavier neutralino can decay to the singlino since the coupling is proportional to $N_{i5} = 0$ for $i > 1$. The NLSP χ_2 is stable for conserved R parity.

However, when the singlet is allowed a weak coupling to the doublets ($\lambda \approx 0$), small mixing between the singlet sector and the SM and MSSM sectors is possible. In this case the a_1 may couple to SM pairs so the a_1 is no longer stable. For $m_{a_1} \approx 10$ GeV, $a_1 \to \tau^+\tau^-$ dominates, with decays to gluon and light quark pairs subdominant. For $m_{h_1} \approx 60$ GeV, $h_1 \to a_1 a_1$ remains dominant with decays to SM pairs, notably $h_1 \to b\bar{b}$, subdominant. Furthermore, the χ_1 can be produced from heavier neutralino decays since singlino mixing with doublinos is allowed. Then the NLSP χ_2 and NNLSP χ_3 are no longer stable against decay to χ_1. Above the threshold $m_{\chi_2} = m_{\chi_1} + m_{a_1} \approx 70$ GeV, $\chi_2 \to \chi_1 a_1$ dominates while below it $\chi_2 \to \chi_1 Z^\star$ dominates. In the latter case, the decay may occur outside the LHC detector effective tracking volume for λ of $\mathcal{O}(10^{-2})$ or less [31]. Above the threshold $m_{\chi_3} = m_{\chi_1} + m_{h_1} \approx 120$ GeV, $\chi_3 \to \chi_1 h_1$ dominates while below it $\chi_3 \to \chi_1 a_1$ and $\chi_3 \to \chi_1 Z^\star$ dominate.

Further information as regards λ and κ can be extracted from the $h_{1,2}$ sum rule [17]

$$m^2_{h_1} + m^2_{h_2} \approx m^2_Z + \frac{1}{2}\kappa v_s(4\kappa v_s + \sqrt{2}A_\kappa) \tag{2}$$

where $v_s \equiv \sqrt{2}\mu_{eff}/\lambda$. For $m_{h_1} = 60$ GeV, $m_{h_2} = 125$ GeV and $\mu_{eff} = 300$ GeV, the sum rule yields $|\kappa/\lambda| \approx 0.176$.

To summarize, we assume an effective MSSM with mostly singlino LSP χ_1 and $m_{\chi_1} \approx 60$ GeV. The a_1 and h_1 are mostly singlet with dominant decays to SM τ pairs and a_1 pairs, respectively. The a_1, h_1, and χ_1 can be produced in neutralino decays. For $m_{\chi_2} \approx 70$ GeV or below and $\lambda < \mathcal{O}(10^{-2})$, the χ_2 decays outside of the effective tracking volume. For $m_{\chi_3} \approx 120$ GeV or above, $\chi_3 \to \chi_1 h_1$ is dominant. Finally, the $h_{1,2}$ mass sum rule yields $|\kappa/\lambda| \approx 0.176$ for $\mu_{\rm eff} = 300$ GeV. These considerations, together with naturalness, inform the parameter ranges in the scan described in the next section.

3 Parameter scan

The parameter scan is performed with NMSSMTools4.4.0 [32–37], probing 10^8 random points. We trade the soft trilinear parameters A_λ, A_κ, A_t for m_P, m_A, X_t, defined by [15,16]

$$m^2_A = \frac{\lambda v_s}{\sin 2\beta}\left(\sqrt{2}A_\lambda + \kappa v_s\right) \tag{3}$$

Table 1 NMSSM parameters and their scan ranges. Additionally, κ is constrained to satisfy $0.125\lambda < |\kappa| < 0.225\lambda$. The point h_{60} ($\kappa = 0.006088$ and $A_\kappa = -1.087$ GeV) is taken from points surviving the scan and is described in Sect. 5

Parameter	Range/Value	h_{60}
λ	(0, 0.1]	0.03505
κ	[−0.01, 0.01]	0.006088
m_A	[500, 1500] GeV	1068. GeV
m_P	[9.9, 10.5] GeV	10.25 GeV
μ_{eff}	[100, 300] GeV	166.7 GeV
$\tan\beta$	[1, 30]	15.49
M_1	$\frac{1}{2}M_2$	80.73 GeV
M_2	[100, 300] GeV	161.5 GeV
M_3	$3M_2$	484.4 GeV
X_t	$[0.8X_t^{\max}, 1.8X_t^{\max}]$	1378. GeV
$m_{\tilde{Q}3_L}$	[350, 550] GeV	546.9 GeV
$m_{\tilde{U}3_R}$	m_{Q3}	546.9 GeV

$$m_P^2 = -\frac{3}{\sqrt{2}}\kappa v_s A_\kappa \tag{4}$$

$$X_t = A_t - \mu_{\text{eff}}/\tan\beta \tag{5}$$

Here m_A (m_P) is the diagonal component of the CP odd doublet (singlet) mass matrix and X_t is the stop mixing parameter.

The parameters scanned are $\lambda, \kappa, m_A, m_P, \mu_{\text{eff}}, \tan\beta, M_2$, X_t, and m_{Q_3}. We fix the gaugino masses M_1 and M_3 with the unification constraints $M_1 = \frac{1}{2}M_2$ and $M_3 = 3M_2$. We further assume $m_{Q_3} = m_{U_3}$. All other squark and soft trilinear parameters are fixed to 1500 GeV, and the slepton mass parameters are fixed to 200 GeV. See Table 1 for scanned parameter ranges.

Motivated by the PQ symmetric NMSSM, we scan small κ and A_κ or equivalently, from Eq. 4, small κ and small m_P. The lower range bound of m_P (9.9 GeV) is informed by the anomalous muon magnetic moment study [25], while the upper bound (10.5 GeV) is informed by the η_b mass spectrum study [26]. Then κ is scanned in the range $-0.01 < \kappa < 0.01$ and is also required to satisfy $0.125\lambda < |\kappa| < 0.225\lambda$ since this requires $m_{h_1} \approx 60$ GeV within several GeV. We scan moderately small λ in the range $0 < \lambda < 0.1$. Since the h_{125} signal strength constraints are applied in the scan, m_A is allowed to go into the effective MSSM decoupling limit $m_A \gg m_Z$ to accommodate the SM-like couplings of the h_{125}.

The neutralino and chargino masses are largely determined by μ_{eff}, M_1 and M_2, which, from naturalness considerations are bounded above in the scan by 300 GeV [12]. At tree level, the stop masses are $m^2_{\tilde{t}_1,\tilde{t}_2} = m^2_{Q_3} + m_t^2 \pm m_t X_t$ for $m_{Q_3} = m_{U_3}$ [15]. Naturalness informs the m_{Q_3} range since light stops are compatible with small fine tuning.

The tree level Higgs mass in the MSSM is bounded by $m_h^2 < m_Z^2 \cos^2 2\beta$, requiring a large loop correction for the h_{125}. In the NMSSM the upper bound on m_h^2 has an additional $\mathcal{O}(\lambda^2 v^2)$ term. The stop mixing parameter X_t partly determines the one loop correction [12]:

$$\delta m_h^2 = \frac{3G_F}{\sqrt{2}\pi^2} m_t^4 \left[\log\left(\frac{m_{\tilde{t}}^2}{m_t^2}\right) + \frac{X_t^2}{m_{\tilde{t}}^2}\left(1 - \frac{X_t^2}{12 m_{\tilde{t}}^2}\right)\right] \tag{6}$$

where the parameter $m_{\tilde{t}}$ is defined by $m_{\tilde{t}}^2 \equiv \frac{1}{2}(m_{\tilde{t}_1}^2 + m_{\tilde{t}_2}^2)$. The correction is strongly dependent on the top mass m_t. In the scan $m_t = 172.5$ GeV.

To allow the large correction required by the h_{125}, but with small $m_{\tilde{t}}$ required by Natural SUSY, the stop mixing X_t is allowed to contribute up to its maximal possible correction at $X_t^{\max} = \sqrt{6} m_{\tilde{t}}$. In the scan NMSSMTools4 calculates the Higgs mass spectrum at one-loop level including external momentum for self-energies and two-loop level excluding external momentum [38,39].

4 Surviving points

The suite of constraints imposed by NMSSMTools4 while scanning includes experimental results from a wide variety of sources, including:

- Anomalous muon magnetic moment Δa_μ measured by BNL E821 [40]
- DM relic density $\Omega_{DM}\hbar^2$ measured by Planck [41], direct DM exclusion by LUX [42]
- B Physics. $b \to s\gamma$, $B \to X_s\mu^+\mu^-$, $B^+ \to \tau^+\nu$, $B_s \to \mu^+\mu^-$, $\Upsilon(1s) \to a\gamma$, $\eta_b(1s)$
- Higgs. LHC h_{125}, LEP $e^+e^- \to Zh$, Tevatron/LHC $t \to bH^+$, NMSSM searches
- SUSY. Tevatron/LHC χ^+, $\tilde{q}$, $\tilde{g}$, $\tilde{e}$, $\tilde{\mu}$, $\tilde{\tau}$ mass constraints, $\tilde{t} \to b\ell\tilde{\nu}$, $\chi^0 c$, and $\tilde{b} \to \chi^0 b$

Loose constraints imposed during the scan require $m_{h_2} \approx 125$ within 3 GeV and impose an upper bound on each h_{125} signal strength χ^2, calculated as in [43]. Of the 10^8 points scanned, 42 survive the constraints imposed during the scan.

Constraints are tightened after the scan. The low mass Higgs sector must satisfy

$$\begin{aligned} 9.9 &< m_{a_1} < 10.5\,\text{GeV} \\ 50 &< m_{h_1} < 70\,\text{GeV} \\ 122 &< m_{h_2} < 128\,\text{GeV} \end{aligned}$$

Finally, the sum of h_{125} signal strength χ^2 are required to satisfy $\sum_i \chi_i^2 < 13$. Of the 42 points surviving the scan constraints, 15 points survive these final constraints.

In order to demonstrate the naturalness of the surviving points, we examine the fine tuning metric $F_{\max} \equiv \max_{a\in A}\left(\frac{\partial(\log m_Z^2)}{\partial(\log a^2)}\right)$ calculated by NMSSMTools4. This metric yields the largest fine tuning over fundamental parameter set A. Surviving points have small fine tuning, $5 < F_{\max} < 10$, light stops $300 < m_{\tilde{t}_1} < 400$ GeV and light gluinos $500 < m_{\tilde{g}} < 650$ GeV. While agreement is not universal on which $F_{\max}$ values characterize low fine tuning [19], studies have considered $F_{\max}$ of order $\mathcal{O}(10^2)$ to be typical for the NMSSM [44] and $\mathcal{O}(10^1)$ to be low fine tuning [22–24,45]. A recent study seeking to establish naturalness as objective, model-independent and predictive concludes that a SUSY model with $F_{\max} < 30$ is natural, while one with $F_{\max} < 10$ is stringently natural [46].

5 Benchmark $\mathbf{h_{60}}$

It has been noted that points surviving the scan represent a Natural NMSSM with slightly broken PQ symmetry. They also exhibit a light pseudoscalar Higgs with $m_{a_1} \approx 10$ GeV, a light scalar Higgs with $m_{h_1} \approx 60$ GeV, a singlino LSP DM candidate with $m_{\chi_1} \approx 60$ GeV annihilating via $\chi_1\chi_1 \to b\bar{b}$, and a light stop with $m_{\tilde{t}_1} \approx 350$ GeV.

The benchmark point h_{60} satisfies the threshold criterion $m_{\chi_3} > m_{h_1} + m_{\chi_1}$ with the largest branching ratio for $\chi_3 \to \chi_1 h_1$ of all surviving points in the scan. The lowest branching ratio for this decay in the surviving points which reach threshold is 65 %, while the highest is 80 %. This ensures production of a_1 from $h_1 \to a_1a_1$ in stop pair events with $\tilde{t}_1 \to \chi_2^+ b \to \chi_3 W b$ or $\tilde{t}_1 \to \chi_3 t$. See the last column of Table 1 for the numerical values of the parameters which define h_{60}. See Fig. 1, generated with PySLHA [47] using the SUSY Les Houches Accord (SLHA) [48,49] file produced by NMSSMTools4, for the mass spectrum and decays in h_{60}.

For components P_{1j}, S_{1j}, N_{ij} of the a_1, h_1, χ_1, χ_2 and χ_3 in h_{60} see Table 2. The LSP χ_1 is dominantly singlino, while the a_1 and h_1 are dominantly singlet. The χ_1 mixing with doublinos and gauginos is small, as is the mixing of the a_1 and h_1 with the doublets. The phenomenology of a singlino LSP at the LHC has been considered in [31,50–57]. The phenomenology of light stops in the NMSSM, and how they avoid exclusion at the LHC, has been recently considered in [58].

For the numerical values of the masses and dominant branching ratios of the low mass spectrum of the h_{60} benchmark, see Table 3. The a_1 and h_1 of the benchmark avoids the LHC search exclusion for straightforward reasons. Both ATLAS and CMS have searched for gluon fusion $gg \to a \to \mu^+\mu^-$ but critically omit the Υ region and therefore cannot exclude $m_{a_1} \approx 10$ GeV [59,60]. ATLAS has searched for gluon fusion $gg \to h \to aa$ for $2m_\tau < m_a < 2m_B$ but does not report limits for $m_h < 100$ GeV [61]. CMS has searched for the same channel but only reports limits for $m_h > 90$ GeV with $m_a < 2m_\tau$ [62] or for the h_{125} with $4 < m_a < 8$ GeV

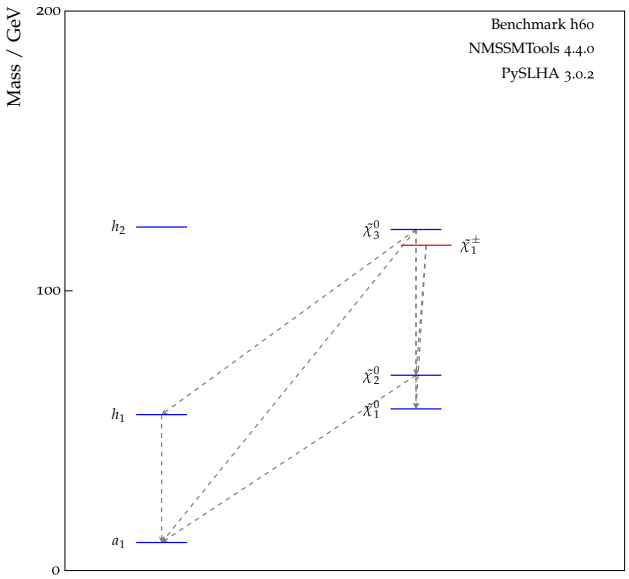

Fig. 1 Masses and decays for the lighter h_{60} benchmark spectrum. Only decays with branching ratios larger than 5 % are shown. Note that the h_2 is mostly decoupled

Table 2 Doublet and singlet components of the a_1, h_1, and gaugino and singlino components of the χ_1, χ_2, χ_3 in h_{60}

Component	a_1	h_1	χ_1	χ_2	χ_3
$P_{11}/S_{11}/N_{i1}$	−0.002	−0.006	0.151	0.882	0.401
$P_{12}/S_{12}/N_{i2}$	0.000	−0.130	−0.054	−0.153	0.679
$P_{13}/S_{13}/N_{i5}$	1.000	0.992	0.981	−0.189	0.045

Table 3 Masses and the two dominant decays of the lighter part of the h_{60} benchmark point spectrum obtained by NMSSMTools4. The column titled "Range" is the mass range of the points surviving all scan constraints

	Range	Mass (GeV)	BR1 (%)	BR2 (%)
a_1	[9.9, 10.4]	10.0	$\tau^+\tau^-$ (81)	gg (16)
h_1	[53, 59]	55.7	a_1a_1 (72)	$b\bar{b}$ (23)
h_2	[122, 123]	122.8	$b\bar{b}$ (65)	$WW^\star$ (17)
χ_1	[54, 60]	57.8	–	–
χ_2	[57, 76]	69.8	$\chi_1 a_1$(75)	$\chi_1 Z^\star$ (25)
χ_3	[107, 136]	121.9	$\chi_1 h_1$ (80)	$\chi_2 Z^\star$ (10)
χ_4	[166, 209]	179.5	$\chi_2 Z$ (80)	$\chi_1 Z$ (14)
χ_5	[225, 254]	236.6	$\chi_1^+ W$ (60)	$\tilde{\nu}\nu$, $\tilde{\ell}\ell$ (38)
χ_1^+	[104, 132]	116.3	$\chi_2 W^\star$ (78)	$\chi_1 W^\star$ (22)
χ_2^+	[225, 255]	237.1	$\ell\tilde{\nu}$, $\tilde{\ell}\nu$ (40)	$\chi_3 W$ (38)
$\tilde{t}_1$	[313, 391]	335.6	$\chi_2^+ b$ (75)	$\chi_3 t$ (15)

[63]. More decisively, the gluon fusion cross sections for a_1 and h_1 production in the benchmark are greatly reduced relative to the h_{125}.

In the neutralino and chargino sector, both ATLAS and CMS have studied $\chi_2\chi_1^+$ production [64–66]. For example, the searches which assume decays to sleptons or to bosons also assume that $m_{\chi_1^+} = m_{\chi_2}$, motivated by models with a bino-like χ_1 and wino-like χ_2 and χ_1^+. But in h_{60} the χ_1 is singlino, and manifestly $m_{\chi_1^+} \neq m_{\chi_2}$. The $\chi_2\chi_1^+$ searches which assume dominant decays to sleptons cannot exclude h_{60} where $m_{\tilde{\ell}} > m_{\chi_1^+}, m_{\chi_2}$. Such searches might be sensitive to $\chi_5\chi_2^+$ events, but here the cross section is reduced and the final states are more complex. Of the searches which assume dominant decays to bosons, only the $W\chi_1 Z\chi_1$ final state case applies. In this case both W and Z are very far off mass shell in h_{60}, in which case it is unlikely that the exclusion can apply.

In the stop sector, both ATLAS and CMS report exclusion. For a summary of the ATLAS results, see [67,68]. For a bibliography of CMS results see [69]. No exclusion is given for the NMSSM, however, and exclusion for simplified models cannot be easily interpreted in the NMSSM context. For example, the analyses which assume $\tilde{t} \to t\chi_1$ with 100 % branching ratio cannot exclude h_{60}, for which this branching ratio is $\mathcal{O}(10^{-3})$. h_{60} does contain $\tilde{t} \to t\chi_3$ with a branching ratio $\mathcal{O}(10^{-1})$, but the subsequent χ_3 decay produces a much more complex final state with less missing energy than assumed by the searches. The stop pair searches which assume $\tilde{t} \to b\chi_1^+$ with 100 % branching ratio assume very specific cases of mass relationships between stops, neutralino and charginos which do not hold in h_{60}. Moreover they assume $\chi_1^+ \to W\chi_1$. But the dominant branching in h_{60} is $\chi_1^+ \to W^\star\chi_2 \to W^\star Z^\star\chi_1$, producing less missing energy, and two gauge bosons which are very far off mass shell in comparison to the search assumptions.

In order to evaluate quantitatively the h_{60} exclusion at LHC Run 1, we run all 16 (3) presently validated ATLAS (CMS) analyses in Checkmate1.2.2 [70–75] on generated h_{60} events. Event simulation of the gluino, stop and chargino/neutralino pair production is carried out with Pythia8.205 [76,77]. The SLHA file produced by NMSSMTools4 for h_{60} is used with Pythia8, which features a dedicated NMSSM model with functionality for SLHA input.

See Table 4 for the exclusion $r_{\max}$, the ratio of the 95 % confidence level lower limit on the h_{60} signal presence to the measured 95 % confidence level limit, of the analyses with maximum sensitivity to h_{60} chargino/neutralino, stop and gluino pair production. Only for gluino pair production is $r_{\max} > 1$, indicating that both ATLAS and CMS have ruled out a gluino with $m_{\tilde{g}} \approx 611$ GeV in h_{60} but neither has ruled out the stop and chargino/neutralino sectors of h_{60}. However, since $m_{\tilde{g}}$ is determined by the gaugino mass M_3, which can be easily increased without otherwise impacting the lower energy h_{60} phenomenology, we simply assume $m_{\tilde{g}} \approx 855$ GeV or greater since this reduces the gluino pair production cross section by a factor of 13 relative to h_{60}.

Table 4 Maximum exclusion $r_{\max}$ determined by Checkmate1 of the analyses most sensitive to $h_{60)}$ of all the validated ATLAS and CMS Run 1 analyses. Note that neither stop nor chargino/neutralino pair production is ruled out for h_{60}

Sample	$r_{\max}$	Analysis	$\int dt\mathcal{L}$ (fb^{-1})
$\chi\bar{\chi}$	0.6	atlas_conf_2013_035	20.7
$\tilde{t}_1\bar{\tilde{t}}_1$	0.5	atlas_conf_2013_061	20.1
$\tilde{g}\tilde{g}$	12.5	atlas_conf_2013_061	20.1
$\chi\bar{\chi}$	0.1	cms_1303_2985	11.7
$\tilde{t}_1\bar{\tilde{t}}_1$	0.6	cms_1502_06031	19.5
$\tilde{g}\tilde{g}$	1.2	cms_1303_2985	11.7

Note that $r_{\max} = 0.6$ for cms_1502_06031, which exhibits a 3σ excess in the low dilepton mass region [78]. If the h_{60} stop mass is reduced such that the stop pair production cross section is enhanced by a factor of 1.5, then this analysis becomes sensitive to h_{60} with the reduced $m_{\tilde{t}} \approx 315$ GeV.

6 Collider signature

Since the stop is relatively light in h_{60}, the cross section for pair production is large and makes cascade production of the a_1 and h_1 accessible at the LHC. Gluon fusion production of a_1 and h_1 is less promising. The reduced tth_1 (tta_1) coupling, which appears in the gluon fusion top loop, is of order $\mathcal{O}(10^{-1})$ ($\mathcal{O}(10^{-5})$) relative to the SM ttH_{SM} coupling for a SM Higgs boson of the same mass.

From Table 3 the decays $\tilde{t}_1 \to \chi_2^+ b$, $\chi_2^+ \to \chi_3 W$, $\chi_3 \to \chi_1 h_1$, and $h_1 \to 2a_1$ proceed with branching ratios of 75, 38, 80, and 72 % respectively, while $\tilde{t}_1 \to \chi_3 t$ proceeds with branching ratio of 15 %. This makes stop pair production with $\tilde{t}_1 \to \chi_2^+ b \to \chi_3 W b$ or $\tilde{t}_1 \to \chi_3 t$ and $\chi_3 \to \chi_1 h_1 \to \chi_1 2a_1$ promising channels for discovery if the a_1 can be successfully reconstructed, for example in the relatively rare but very clean $a_1 \to \mu^+\mu^-$ channel. In h_{60} this decay proceeds with a branching ratio of 0.3 %. These remarks also apply to stop pairs produced in gluino pair production with $\tilde{g} \to \tilde{t}_1 t$.

In h_{60} stop pair production, the cascade dominantly contains two top quarks. In gluino pair production it dominantly contains four top quarks. These are strong handles on any potential background. Some top pair $t\bar{t}$ background may be irreducible, but other backgrounds should be negligible.

We now describe a targeted study of the sensitivity to h_{60} at the LHC. Signal events are generated with Pythia8 as described in Sect. 5. Background $t\bar{t}$ events are also generated in Pythia8. Fast detector simulation is performed with Delphe3.2.0 [71]. The Delphes3 detector card for CMS is

modified to reproduce the tight electron, tight muon and b tag efficiencies reported by CMS [79–81]. The signal selection seeks the decay $a_1 \to \mu^+\mu^-$ in gluino and stop pair events and employs a standard selection for semileptonic top pair events, together with a selection for $a_1 \to \mu^+\mu^-$, in which one top quark decays via $t \to bW \to b\ell\nu$ and the other via $t \to bW \to bqq'$. The requirements for the Run 1 analysis are these:

- Exactly one tight electron with $E_T > 25$ GeV and no isolation requirement
- Missing transverse energy $E_T^{miss} > 85$ GeV
- Four or more jets with $E_T > 20$ GeV, at least two of which are b-tagged
- Two or more tight muons with $p_T > 2$ GeV, no isolation requirement and $d_0/\sigma_{d_0} < 5$
- Zero net charge and $9.7 < m_{\mu^+\mu^-} < 10.3$ GeV in the leading and subleading muons

The a_1 candidate is then reconstructed from the leading and subleading muons. The muon azimuthal impact parameter significance requirement $d_0/\sigma_{d_0} < 5$ ensures that the muons are consistent with prompt production.

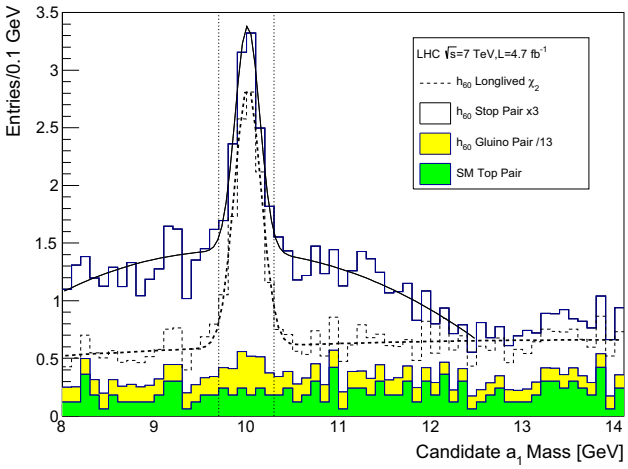

Fig. 2 Reconstructed candidate $a_1 \to \mu^+\mu^-$ mass distribution after full signal selection assuming h_{60} ($\times 3$ for $\tilde{t}_1\bar{\tilde{t}}_1$ and $/13$ for $\tilde{g}\tilde{g}$) at the LHC for $\sqrt{s} = 7$ TeV and $\int dt\mathcal{L} = 4.7$ fb^{-1}. Also shown (dashed) is a variation of h_{60} in which the χ_2 decays outside of the effective tracking volume. The fits employ a Gaussian signal model and a polynomial background model

For the Run 2 analysis, we assume $\sqrt{s} = 14$ TeV and $\int dt\mathcal{L} = 300$ fb^{-1}. We use the Delphes3 simulation with mean pileup 50. The selection is identical to the Run 1 analysis except that the electron, jet, and muon thresholds are raised to 30, 30 and 4 GeV, respectively.

After full signal selection, the SM top background is nearly negligible. Multiple jet events produced by QCD have not been simulated, but with the nominal selection this background is expected to be very small. In data, the nonpeaking h_{60} events in the candidate a_1 distribution can be mistaken for QCD multijets events, however, so these are considered background in the significance calculation. In the SM top background, the candidate a_1 muons originate from τ lepton, D meson or B meson decays. In the nonpeaking h_{60} events, they originate either from SM τ, B or D decay or from NMSSM $a_1 \to \tau_\mu\tau$, $\chi_2 \to \chi_1\mu^+\mu^-$, $\chi^+ \to \chi\mu\nu$, or $\chi^+ \to \mu\tilde{\nu}$.

The proportion of peaking to nonpeaking signal events is sensitive to the details of h_{60}. For example, if the slepton masses are raised above the threshold for decay from χ_2^+, then the peaking signal is enhanced and the nonpeaking signal is reduced. Similarly, if the branching ratio for $\chi_2 \to \chi_1 a_1$ is raised at the expense of $\chi_2 \to \chi_1 Z^\star$, the peaking signal is enhanced and the nonpeaking signal is reduced. Finally, if the χ_2 width is sufficiently small, its decay vertices may lie outside the effective tracking volume, making nonpeaking background from χ_2 effectively invisible.

Pythia8 is a leading order generator, but next to leading order cross sections obtained by the LHC SUSY Working Group [82,83] are used to normalize the event yields. See Figure 2 for the reconstructed a_1 mass distribution after full signal selection, where the distribution for a variation of h_{60} in which the χ_2 decays outside of the tracking volume is also shown. See Table 5 for expected peaking and nonpeaking event yields and signal significances after full selection for Runs 1 and 2 at the LHC. A targeted h_{60} signal selection yields sensitivity even at the LHC Run 1.

Table 5 NLO cross sections for $\tilde{t}_1\bar{\tilde{t}}_1$ and $t\bar{t}$ production at the LHC in Runs 1 ($\sqrt{s} = 7, 8$ TeV) and 2 ($\sqrt{s} = 14$ TeV). Also shown are the expected yields for peaking events (N_p), yields for nonpeaking events (N_n) and signal significances after the full signal selection described in the text. For $\sqrt{s} = 7$ TeV, we show in parentheses the yields and the significance for a variation of h_{60} in which the χ_2 decays outside of the effective tracking volume

Process	Run 1: $\mathcal{L} = 5$ fb^{-1}			Run 1: $\mathcal{L} = 20$ fb^{-1}			Run 2: $\mathcal{L} = 300$ fb^{-1}		
	σ_{7T} (pb)	N_n	N_p	σ_{8T} (pb)	N_n	N_p	σ_{14T} (pb)	N_n	N_p
SM $t\bar{t}$	173.6	1.6	0	247.7	8.5	0	966.0	286.0	0
h_{60} $\tilde{t}_1\bar{\tilde{t}}_1$	0.7	2.6 (0.8)	2.2 (2.5)	1.1	20.1	19.2	5.9	892.5	647.9
$S/\sqrt{B}$	1.0(1.6)			3.6			18.9		

The advantages of the International Linear Collider (ILC) for studying low mass NMSSM Higgs bosons has been noted in [15]. At the ILC, the standard Higgsstrahlung production channel $e^+e^- \to Zh_1$ is suppressed in the NMSSM due to the measured SM-like $h_{125} \to ZZ^\star$ signal strength and the NMSSM coupling sum rule $\sum_{1=1}^{3} \xi^2_{ZZh_i} = 1$ [14]. Instead, in h_{60} we note the possibility of resonant production $e^+e^- \to a_1h_1$, with cross section of several hundred picobarns at $\sqrt{s} = m_Z$. For $\sqrt{s} = 500$ GeV, pair production of all neutralinos and all charginos is accessible with cross sections nearing a picobarn, as well as a_1h_1 and Zh_2 production cross sections of about a hundred femtobarns.

In h_{60} the Za_1h_1 coupling is small enough to have evaded LEP searches [84,85] but large enough to be produced copiously at the ILC running on the Z pole. The ILC sensitivity to h_{60} in operating scenarios described in [86] defined by beam polarization, luminosity, and $\sqrt{s}$ and will be evaluated in a forthcoming companion study.

7 Conclusion

We have reviewed the motivation for a natural NMSSM with a slightly broken PQ symmetry and a lightly coupled singlet featuring a light singlet pseudoscalar a_1, a light singlet scalar h_1, and a light singlino LSP χ_1 DM candidate annihilating via $\chi_1\chi_1 \to b\bar{b}$.

A random parameter space scan is performed subject to a full suite of experimental constraints, including the anomalous muon magnetic moment, the DM relic density and collider searches. Surviving points are characterized by low fine tuning, and abundant pseudoscalar a_1 production identifies the benchmark point h_{60}. In addition this benchmark features light stops and light higgsinos, all characteristic of Natural SUSY.

The benchmark avoids the current LHC exclusion limits. For the a_1 and h_1, this is due to the reduced gluon fusion cross sections. For other SUSY searches, this is primarily due to the search assumption that stops, neutralinos, and charginos will decay directly to the LSP χ_1 with no intermediate SUSY particles in the decay chain. But in the h_{60} benchmark the χ_1 is singlino and couples weakly to the rest of SUSY. Thus due to the light mass spectrum the decay chains can contain many intermediate SUSY particles, making the final states more complex with less missing energy than in the simplified search scenarios.

Finally, we report that the potentially fruitful discovery channels at the LHC for the benchmark considered are stop and gluino pair production with either $\tilde{t}_1 \to \chi_2^+ b \to \chi_3 Wb$ or $\tilde{t}_1 \to \chi_3 t$ and $\chi_3 \to \chi_1 h_1 \to \chi_1 a_1 a_1$. We conclude with a fast simulation study that with a targeted signal selection the LHC may already be sensitive to h_{60} in Run 1. We have also pointed out the possibility to observe at the ILC resonant $e^+e^- \to a_1h_1$ at $\sqrt{s} = m_Z$ and pair production of all neutralinos and charginos at $\sqrt{s} = 500$ GeV.

Acknowledgments The author thanks M. Muhlleitner for discussion of the Higgs mass calculation in NMSSMTools4, Tao Liu for feedback on fine tuning and the PQ symmetric NMSSM, and the Alder Institute for High Energy Physics for financial support.

Open Access This article is distributed under the terms of the Creative Commons Attribution 4.0 International License (http://creativecommons.org/licenses/by/4.0/), which permits unrestricted use, distribution, and reproduction in any medium, provided you give appropriate credit to the original author(s) and the source, provide a link to the Creative Commons license, and indicate if changes were made.
Funded by SCOAP[3].

References

1. G. Aad et al., Observation of a new particle in the search for the Standard Model Higgs boson with the ATLAS detector at the LHC. Phys.Lett. **B716**, 1–29 (2012). arXiv:1207.7214
2. S. Chatrchyan et al., Observation of a new boson at a mass of 125 GeV with the CMS experiment at the LHC. Phys. Lett. **B716**, 30–61 (2012). arXiv:1207.7235
3. M.S. Carena, H.E. Haber, Higgs boson theory and phenomenology. Prog. Part. Nucl. Phys. **50**, 63–152 (2003). arXiv:hep-ph/0208209
4. G. Aad et al., Combined measurement of the Higgs Boson Mass in pp and 8 TeV with the ATLAS and CMS Experiments. Phys. Rev. Lett. **114**, 191803 (2015). arXiv:1503.07589
5. V. Khachatryan et al., Precise determination of the mass of the Higgs boson and tests of compatibility of its couplings with the standard model predictions using proton collisions at 7 and 8 TeV. Eur. Phys. J. C **75**(5), 212 (2015). arXiv:1412.8662
6. G. Aad et al., Measurements of the Higgs boson production and decay rates and coupling strengths using pp TeV in the ATLAS experiment (2015). arXiv:1507.04548
7. G. Aad et al., Study of the spin and parity of the Higgs boson in diboson decays with the ATLAS detector. **1506**, 05669 (2015)
8. V. Khachatryan et al., Constraints on the spin-parity and anomalous HVV couplings of the Higgs boson in proton collisions at 7 and 8 TeV. Phys. Rev. D **92**(1), 012004 (2015). arXiv:1411.3441
9. V. Khachatryan et al., Limits on the Higgs boson lifetime and width from its decay to four charged leptons (2015). arXiv:1507.06656
10. S.P. Martin, A supersymmetry primer (1997). hep-ph/9709356
11. M. Dine, Naturalness under. Stress **1501**, 01035 (2015)
12. M. Papucci, J.T. Ruderman, A. Weiler, Natural SUSY Endures. JHEP, **1209**, 035 (2012). arXiv:1110.6926
13. M. Maniatis, The next-to-minimal supersymmetric extension of the standard model reviewed. Int. J. Mod. Phys. **A25**, 3505–3602 (2010). arXiv:0906.0777
14. U. Ellwanger, C. Hugonie, A.M. Teixeira, The next-to-minimal supersymmetric standard model. Phys. Rept. **496**, 1–77 (2010). arXiv:0910.1785
15. D.J. Miller, R. Nevzorov, P.M. Zerwas, The higgs sector of the next-to-minimal supersymmetric standard model. Nucl. Phys. B **681**(1–2), 3–30 (2004)
16. U. Ellwanger, Higgs Bosons in the next-to-minimal supersymmetric standard model at the LHC. Eur. Phys. J. **C71**, 1782 (2011). arXiv:1108.0157
17. D.J. Miller, R. Nevzorov, The Peccei-Quinn axion in the next-to-minimal supersymmetric standard model (2003). arXiv:hep-ph/0309143

18. L.J. Hall, T. Watari, Electroweak supersymmetry with an approximate U(1)(PQ). Phys. Rev. D **70**, 115001 (2004). arXiv:hep-ph/0405109
19. C. Philip, Schuster and Natalia Toro. Persistent fine-tuning in supersymmetry and the NMSSM (2005). arXiv:hep-ph/0512189
20. R. Barbieri, L.J. Hall, A.Y. Papaioannou, D. Pappadopulo, V.S. Rychkov, An alternative NMSSM phenomenology with manifest perturbative unification. JHEP, **03**, 005 (2008). arXiv:0712.2903
21. K. Choi, S.H. Im, K.S. Jeong, M.S. Seo, Higgs phenomenology in the Peccei-Quinn invariant NMSSM. JHEP, **1401**, 072 (2014). arXiv:1308.4447
22. R. Dermisek, J.F. Gunion, Escaping the large fine tuning and little hierarchy problems in the next to minimal supersymmetric model and $h \to aa$ decays. Phys. Rev. Lett. **95**, 041801 (2005). arXiv:hep-ph/0502105
23. R. Dermisek, J.F. Gunion, The NMSSM Close to the R-symmetry limit and naturalness in $h \to aa$ decays for $m_a < 2m_b$. Phys. Rev. D **75**, 075019 (2007). arXiv:hep-ph/0611142
24. R. Dermisek, J.F. Gunion, The NMSSM solution to the fine-tuning problem, precision electroweak constraints and the largest LEP Higgs event excess. Phys. Rev. **D76**, 095006 (2007). arXiv:0705.4387
25. J.F. Gunion, A Light CP-odd Higgs boson and the muon anomalous magnetic moment. JHEP, **0908**, 032 (2009). arXiv:0808.2509
26. F. Domingo, U. Ellwanger, M.A. Sanchis-Lozano, Bottomoniom spectroscopy with mixing of eta(b) states and a light CP-odd Higgs. Phys. Rev. Lett. **103**, 111802 (2009). arXiv:0907.0348
27. R. Dermisek, J.F. Gunion, New constraints on a light CP-odd Higgs boson and related NMSSM Ideal Higgs Scenarios. Phys. Rev. **D81**, 075003 (2010). arXiv:1002.1971
28. J. March-Russell, J. Unwin, S.M. West, Closing in on asymmetric dark matter I: model independent limits for interactions with quarks. JHEP, **1208**, 029 (2012). arXiv:1203.4854
29. S. Schael et al., Search for neutral MSSM Higgs bosons at LEP. Eur. Phys. J. **C47**, 547–587 (2006). arXiv:hep-ex/0602042
30. F. Franke, H. Fraas, Neutralinos and Higgs bosons in the next-to-minimal supersymmetric standard model. Int. J. Mod. Phys. A **12**, 479–534 (1997). arXiv:hep-ph/9512366
31. U. Ellwanger, C. Hugonie, Neutralino cascades in the (M+1)SSM. Eur. Phys. J. C **5**, 723–737 (1998). arXiv:hep-ph/9712300
32. U. Ellwanger, J.F. Gunion, C. Hugonie, NMHDECAY: A Fortran code for the Higgs masses, couplings and decay widths in the NMSSM. JHEP **0502**, 066 (2005). arXiv:hep-ph/0406215
33. U. Ellwanger, C. Hugonie, NMHDECAY 2.0: An Updated program for sparticle masses, Higgs masses, couplings and decay widths in the NMSSM. Comput. Phys. Commun. **175**, 290–303 (2006). arXiv:hep-ph/0508022
34. G. Belanger, F. Boudjema, C. Hugonie, A. Pukhov, A. Semenov, Relic density of dark matter in the NMSSM. JCAP **0509**, 001 (2005). arXiv:hep-ph/0505142
35. U. Ellwanger, C. Hugonie, NMSPEC: A Fortran code for the sparticle and Higgs masses in the NMSSM with GUT scale boundary conditions. Comput. Phys. Commun. **177**, 399–407 (2007). arXiv:hep-ph/0612134
36. D. Das, U. Ellwanger, A.M. Teixeira, NMSDECAY: A Fortran Code for Supersymmetric Particle Decays in the Next-to-Minimal Supersymmetric Standard Model. Comput. Phys. Commun. **183**, 774–779 (2012). arXiv:1106.5633
37. M. Muhlleitner, A. Djouadi, Y. Mambrini, SDECAY: A Fortran code for the decays of the supersymmetric particles in the MSSM. Comput. Phys. Commun. **168**, 46–70 (2005). arXiv:hep-ph/0311167
38. G. Degrassi, P. Slavich, On the radiative corrections to the neutral Higgs boson masses in the NMSSM. Nucl. Phys. **B825**, 119–150 (2010). arXiv:0907.4682
39. F. Staub, P. Athron, U. Ellwanger, R. Grober, M. Muhlleitner, P. Slavich, A. Voigt, Higgs mass predictions of public NMSSM spectrum generators. **1507**, 05093 (2015)
40. G.W. Bennett et al., Final Report of the Muon E821 anomalous magnetic moment measurement at BNL. Phys. Rev. **D73**, 072003 (2006). arXiv:hep-ex/0602035
41. P.A.R. Ade Planck et al., Results. XVI. Cosmological parameters. Astron. Astrophys. **571**(A16), 2014 (2013). arXiv:1303.5076
42. D.S. Akerib et al., First results from the LUX dark matter experiment at the Sanford Underground Research Facility. Phys. Rev. Lett. **112**, 091303 (2014). arXiv:1310.8214
43. G. Belanger, B. Dumont, U. Ellwanger, J.F. Gunion, S. Kraml, Global fit to Higgs signal strengths and couplings and implications for extended Higgs sectors. Phys. Rev. **D88**, 075008 (2013). arXiv:1306.2941
44. M.Y. Binjonaid, S.F. King, Naturalness of scale-invariant NMSSMs with and without extra matter. Phys. Rev. D **90**(5), 055020 (2014). arXiv:1403.2088
45. L.J. Hall, D. Pinner, J.T. Ruderman, A Natural SUSY Higgs Near 126 GeV. JHEP, **04**, 131 (2012). arXiv:1112.2703
46. H. Baer, V. Barger, M. Savoy, Upper bounds on sparticle masses from naturalness or how to disprove weak scale supersymmetry. **1509**, 02929 (2015)
47. A. Buckley, PySLHA: a Pythonic interface to SUSY Les Houches Accord data. (2013). arXiv:1305.4194
48. P.Z. Skands et al., SUSY Les Houches accord: Interfacing SUSY spectrum calculators, decay packages, and event generators. JHEP **07**, 036 (2004). arXiv:hep-ph/0311123
49. B.C. Allanach et al., SUSY Les Houches Accord 2. Comput. Phys. Commun. **180**, 8–25 (2009). arXiv:0801.0045
50. J.F. Gunion, D. Hooper, B. McElrath, Light neutralino dark matter in the NMSSM. Phys. Rev. D **73**, 015011 (2006). arXiv:hep-ph/0509024
51. J. Cao, C. Han, L. Wu, P. Wu, J.M. Yang, A light SUSY dark matter after CDMS-II, LUX and LHC Higgs data. JHEP, **1405**, 056 (2014). arXiv:1311.0678
52. T. Han, Z. Liu, S. Su, Light neutralino dark matter: direct/indirect detection and collider searches. JHEP, **1408**, 093 (2014). arXiv:1406.1181
53. U. Ellwanger, A.M. Teixeira, NMSSM with a singlino LSP: possible challenges for searches for supersymmetry at the LHC. JHEP **1410**, 113 (2014). arXiv:1406.7221
54. J.S. Kim, T.S. Ray, The higgsino-singlino world at the large hadron collider. Eur. Phys. J. **C75**, 40 (2015). arXiv:1405.3700
55. C. Han, D. Kim, S. Munir, M. Park, $\mathcal{O}(1)$ GeV dark matter in SUSY and a very light pseudoscalar at the LHC. (2015). arXiv:1504.05085
56. P. Draper, T. Liu, C.E.M. Wagner, L.T. Wang, H. Zhang, Dark light Higgs. Phys. Rev. Lett. **106**, 121805 (2011). arXiv:1009.3963
57. M. Casolino, T. Farooque, A. Juste, T. Liu, M. Spannowsky, Probing a light CP-odd scalar in di-top-associated production at the LHC. (2015). arXiv:1507.07004
58. J. Beuria, A. Chatterjee, A. Datta, S.K. Rai, Two Light Stops in the NMSSM and the LHC. (2015). arXiv:1505.00604
59. A Search for Light CP-Odd Higgs Bosons Decaying to mu+ mu- in ATLAS. Technical Report ATLAS-CONF-2011-020 (CERN, Geneva, 2011)
60. Search for a light pseudoscalar boson in the dimuon channel. Technical Report CMS-PAS-HIG-12-004 (CERN, Geneva, 2012)
61. G. Aad et al., Search for Higgs bosons decaying to aa 8 TeV with the ATLAS experiment. (2015). arXiv:1505.01609
62. V. Khachatryan et al., A search for pair production of new light bosons decaying into muons. (2015). arXiv:1506.00424
63. V. Khachatryan et al., Search for a very light NMSSM Higgs boson produced in decays of the 125 GeV scalar boson and decaying into τ 8 TeV. (2015). arXiv:1510.06534

64. V. Khachatryan et al., Searches for electroweak production of charginos, neutralinos, and sleptons decaying to leptons and W, Z, and Higgs bosons in pp collisions at 8 TeV. Eur. Phys. J. C **74**(9), 3036 (2014). arXiv:1405.7570
65. V. Khachatryan et al., Searches for electroweak neutralino and chargino production in channels with Higgs, Z, and W bosons in pp collisions at 8 TeV. Phys. Rev. D **90**(9), 092007 (2014). arXiv:1409.3168
66. G. Aad et al., Search for the electroweak production of supersymmetric particles in $\sqrt{s}$ collisions with the ATLAS detector. (2015). arXiv:1509.07152
67. G. Aad et al., ATLAS Run 1 searches for direct pair production of third-generation squarks at the Large Hadron Collider. (2015). arXiv:1506.08616
68. G. Aad et al., Summary of the searches for squarks and gluinos using $\sqrt{s} = 8$ TeV pp collisions with the ATLAS experiment at the LHC. (2015). arXiv:1507.05525
69. Commissioning the performance of key observables used in SUSY searches with the first 13 TeV data. (2015)
70. M. Drees, H. Dreiner, D. Schmeier, J. Tattersall, J. Soo Kim, CheckMATE: confronting your favourite new physics model with LHC data. Comput. Phys. Commun. **187**, 227–265 (2014). arXiv:1312.2591
71. J. de Favereau, C. Delaere, P. Demin, A. Giammanco, V. Lemaetre, A. Mertens, M. Selvaggi, DELPHES 3, a modular framework for fast simulation of a generic collider experiment. JHEP **02**, 057 (2014). arXiv:1307.6346
72. M. Cacciari, G.P. Salam, G. Soyez, FastJet user manual. Eur. Phys. J. **C72**, 2012 (1896). arXiv:1111.6097
73. M. Cacciari, G.P. Salam, Dispelling the N^3 myth for the k_t jet-finder. Phys. Lett. B **641**, 57–61 (2006). arXiv:hep-ph/0512210
74. M. Cacciari, G.P. Salam, G. Soyez, The Anti-k(t) jet clustering algorithm. JHEP, **04**, 063 (2008). arXiv:0802.1189
75. A.L. Read, Presentation of search results: the CL(s) technique. J. Phys. **G28**, 2693–2704 (2002)
76. T. Sjostrand, S. Mrenna, P.Z. Skands, A brief introduction to PYTHIA 8.1. Comput. Phys. Commun. **178**, 852–867 (2008). arXiv:0710.3820
77. T. Sjostrand, S. Mrenna, P.Z. Skands, PYTHIA 6.4 physics and manual. JHEP, **0605**, 026 (2006). arXiv:hep-ph/0603175
78. V. Khachatryan et al., Search for physics beyond the standard model in events with two leptons, jets, and missing transverse momentum in pp collisions at sqrt(s) = 8 TeV. JHEP, **04**, 124 (2015). arXiv:1502.06031
79. Electron performance with 19.6 fb^{-1} TeV with the CMS detector. (2013)
80. Performance of b tagging at sqrt(s)=8 TeV in multijet, ttbar and boosted topology events. Technical Report CMS-PAS-BTV-13-001 (CERN, Geneva, 2013)
81. CMS collaboration, Performance of CMS muon reconstruction in pp collision events at $\sqrt{s} = 7$ TeV. J. Instrum. **7**, P10002 (2012). arXiv:1206.4071 (CMS-MUO-10-004. CERN-PH-EP-2012-173. Submitted to the Journal of Instrumentation)
82. M. Kramer, A. Kulesza, R. van der Leeuw, M. Mangano, S. Padhi, T. Plehn, X. Portell, Supersymmetry production cross sections in pp TeV. (2012). arXiv:1206.2892
83. C. Borschensky, M. Kramer, A. Kulesza, M. Mangano, S. Padhi, T. Plehn, X. Portell, Squark and gluino production cross sections in pp collisions at $\sqrt{s} = 13$, 14, 33 and 100 TeV. Eur. Phys. J. C **74**(12), 3174 (2014). arXiv:1407.5066
84. R. Barate et al., Search for the standard model Higgs boson at LEP. Phys. Lett. **B565**, 61–75 (2003). arXiv:hep-ex/0306033
85. G. Alexander et al., Search for neutral Higgs bosons in Z^0 decays using the OPAL detector at LEP. Z. Phys. C **73**, 189–199 (1997)
86. T. Barklow, J. Brau, K. Fujii, J. Gao, J. List, N. Walker, K. Yokoya, ILC operating scenarios. **1506**, 07830 (2015)